An Engineered Disulfide Cross-Link Accelerates the Refolding Rate of Calcium-Free Subtilisin by 850-Fold†

Susan Strausberg,‡ Patrick Alexander,‡ Lan Wang,‡ Travis Gallagher,§ Gary Gilliland,§ and Philip Bryan*,‡

Center for Advanced Research in Biotechnology of the Maryland Biotechnology Institute, and the National Institutes of Standards and Technology, 9600 Gudelsky Drive, Rockville, Maryland 20850

Received April 21, 1993; Revised Manuscript Received July 19, 1993®

ABSTRACT: The mature form of subtilisin is an unusual example of a monomeric protein with a high kinetic barrier to folding and unfolding. Using site-directed mutagenesis of subtilisin BPN′, we are attempting to determine the physical and energetic nature of the kinetic barrier. The high-affinity calcium-binding site A has been shown to create a large enthalpic barrier to unfolding. Removing the calcium-binding site A from subtilisin by deleting amino acids 75–83 greatly accelerates both unfolding and refolding reactions. Here a disulfide cross-link is introduced between residues 22 and 87 in Δ75–83 subtilisin. This was done to probe the conformational entropy of the transition state for folding. The 1.8-Å X-ray structure of this mutant and the effects of the cross-link on the kinetics of unfolding and refolding are reported. Consistent with an expected loss of entropy of the unfolded protein due to the cross-link, the disulfide accelerates folding relative to the uncross-linked form. The magnitude of the acceleration of folding rate (700–850-fold at 25 °C) indicates that residues 22 and 87 are ordered in the transition state such that the disulfide does not affect its total entropy. Although early organization of structure around amino acids 22 and 87 greatly accelerates folding, we do not know whether the early folding of this region is a highly populated folding pathway in the absence of the cross-link. The slow step in the Δ75–83 subtilisin folding reaction may be forming initial structures capable of propagating the folding reaction. Any mutation (or ionic condition) which stabilizes a native-like topology may therefore accelerate its folding rate.

Most of the research on the energetics of protein folding has concentrated on relatively small, globular proteins, which readily unfold and refold. Subtilisin, the 275-amino-acid serine protease from *Bacillus amyloliquefaciens*, is a very stable protein on the upper limit in size for a cooperative folding unit.[1] While its folding is governed by the same chemical forces as those of smaller proteins, the folding reaction of subtilisin manifests some unusual features. The in vitro folding of subtilisin is extremely slow, and recent experiments have demonstrated that a high kinetic barrier exists between the folded and unfolded states of subtilisin (Bryan et al., 1992). The high kinetic barrier is apparently one of the reasons that the in vivo biosynthesis of native subtilisin depends on a 77-amino-acid propeptide, which is eventually cleaved from the N-terminus of subtilisin to create the mature form of the enzyme (Ikemura et al., 1987; Strausberg et al., 1993; Zhu et al., 1989). A high activation barrier to folding has also been observed for another bacterial protease, α-lytic protease, which uses a 166-amino-acid propeptide to catalyze its folding reaction (Baker et al., 1992a,b).

Using variations of S221C subtilisin,[2] we are attempting to understand the energetics of catalyzed (Strausberg et al., 1993) and uncatalyzed (Bryan et al., 1992) subtilisin folding. A major part of the kinetic problem to folding involves the formation of the high-affinity calcium-binding site A. Unfolded subtilisin, when returned to native conditions, collapses into a stable and highly structured intermediate state which is not converted to the native state after more than 1 week at 15 °C (Eder et al., 1993). Removal of site A by deleting amino acids 75–83 greatly accelerates the rates of folding and unfolding (Bryan et al., 1992; Gallagher et al., 1993).

Residues 75–83 form a loop which interrupts the last turn of a 14-residue α-helix involving amino acids 63–85 (McPhalen & James, 1988). Four of the six ligands to the calcium are provided by this loop. Deletion of amino acids 75–83 creates an uninterrupted helix and abolishes the calcium-binding potential at site A (Figure 1). X-ray crystallography has shown that, except for the region of the deleted calcium-binding loop, the structure of the mutant and wild-type protein are remarkably similar, considering the size of the deletion (Bryan et al., 1992; Gallagher et al., 1993). The structures of subtilisin with and without the deletion superimpose with an rms difference between 261 Cα positions of 0.17 Å. Diffuse difference density and higher temperatures factors indicate some disorder in the newly exposed residues adjacent to the deletion. The N-terminus of the wild-type protein lies beside the site A loop, furnishing one calcium coordination ligand, the side-chain oxygen of Q2. In Δ75–83 subtilisin, the loop is gone, leaving residues 1–4 disordered, but the helix is

† This work was supported by NIH Grant GM42560.

* Corresponding author.
‡ Center for Advanced Research in Biotechnology.
§ National Institutes of Standards and Technology.

® Abstract published in *Advance ACS Abstracts*, September 1, 1993.

[1] Abbreviations: CD, circular dichroism; Dns-BBA, (3-*N*-dansylaminobenzene)boronic acid; Δ75–83 subtilisin, subtilisin BPN′ with a deletion of amino acids 75–83; $\Delta H^{\ddagger}$, enthalpy for formation of the transition state for folding; DSC, differential scanning calorimetry; EDTA, disodium salt of ethylene diaminetetraacetic acid; HEPES, *N*-(2-hydroxyethyl)piperazine-*N*′-2-ethanesulfonic acid; [P], protein concentration; rms, root mean square; sAAPFna, succinyl-L-Ala-L-Ala-L-Pro-L-Phe-*p*-nitroanilide; Tris, tris(hydroxymethyl)aminomethane; $t_{1/2}$, half-life for a kinetic experiment; wt, wild type.

[2] S221C denotes the change of serine 221 to cysteine. This mutation reduces proteolytic activity to a level that is measurable but no longer problematic for folding studies (Abrahmsen et al., 1991; Bryan et al., 1992; Polger & Bender, 1966). The specific activities of all S221C mutants discussed here are similar (SA ≈ 0.025 unit/mg at 25 °C, pH 8.0, using the synthetic substrate sAAPFna).

0006-2960/93/0432-10371$04.00/0

FIGURE 1: X-ray crystal structure of Δ73–83 subtilisin with the 22–87 disulfide cross-link. α-carbon plot shows the position of the 22–87 disulfide cross-link. Dotted spheres show the position of the weak ion-binding site B and the former position of the A-site. The A-site looop (dashed line) is absent in this mutant. N- and C-termini are indicated. The first five amino acids of the N-terminus are disordered (dotted line). The structure was determined for subtilisin S22 as defined in Table I.

uninterrupted and shows normal helical geometry over its entire length (Figure 1).

While Δ75–83 subtilisin can fold efficiently without the participation of the propeptide, its rate of folding is on the order of hours^{-1} at low ionic strength. In the work described here, a disulfide cross-like between residues 22 and 87 was introduced into the Δ75–83 subtilisin. The basic rationale was to probe the nature of the transition state for folding Δ75–83 subtilisin. If the amino acids 22 and 87 are ordered in the transition state for folding, then one would expect that the cross-link would accelerate the rate of folding because it would selectively decrease the entropy of the unfolded state relative to that of the transition state. In this paper, the X-ray structure of this subtilisin is reported and the energetic effects of the disulfide on the folding reaction are examined.

MATERIALS AND METHODS

Cloning and Expression. The subtilisin gene from *Bacillus amyloliquefaciens* (subtilisin BPN′) has been cloned, sequenced, and expressed at high levels from its natural promoter sequences in *Bacillus subtilis* (Vasantha et al., 1984; Wells et al., 1983). All mutant genes were recloned into a pUB110-based expression plasmid and used to transform *B. subtilis*. The *B. subtilis* strain used as the host contains a chromosomal deletion of its subtilisin gene and therefore produces no background wild-type activity. Oligonucleotide mutagenesis was carried out as previously described (Bryan et al., 1986a). S221C was expressed in a 1.5-L New Brunswick fermentor at a level of ~100 mg of the correctly processed mature form per liter. The addition of wild-type subtilisin to promote production of the mature form of S221C subtilisin was not required in our bacillus host strain, as was the case for Abrahmsen et al., 1991.

Protein Purification and Characterization. Variant subtilisins were purified and verified for homogeneity essentially as described by Bryan et al. (1986a). C221 mutant subtilisins not containing the disulfide cross-link were repurified on a sulfhydryl-specific mercury affinity column (Affi-gel 501, Bio-Rad). Assays of peptidase activity were performed by monitoring the hydrolysis of a sAAPFna as described by DelMar et al (1979). The [P] was determined using $P^{0.1\%}$ = 1.17 at 280 nm (Pantoliano et al., 1989). For variants which contain the Y217K change, the $P^{0.1\%}$ at 280 nm was calculated to be 1.12 (or 0.96 × wt) on the basis of the loss of one Tyr residue.

Table I: Subtilisin Mutations[a]

	S221C	Δ75–83	G169A	T22C-S87C
S12	+	–	–	–
S15	+	+	–	–
S22	+	+	–	+
S23	+	+	+	–
S29	+	+	+	+

[a] The plus signs show that a subtilin contains a particular mutation.[3] A shorthand for denoting amino acid substitutions employs the single letter amino acid code as follows: S221C denotes the change of serine 221 to cysteine. All variants contain the stabilizing mutations M50F, Y217K, and N218S. X-ray crystal structures of S12, S15, and S22 have been determined to 1.8 Å. Coordinates of the refined structures are in the Protein Data Bank: 1sud (S12) and 1suc (S15); S22 is not yet assigned an identifier.

Circular Dichroism. CD spectra of mutant subtilisins were measured using a JASCO 720 spectropolarimeter. In thermal denaturation experiments, protein samples at a concentration of 1 μM were monitored at 222 nm while being heated at a uniform rate using a 1-cm-pathlength jacketed cuvette. Temperature was increased with a circulating water bath, interfaced with a NESLAB temperature programmer. Heating rates were either 0.5 or 1 °C/min. Derivative melting curves were calculated using KaleidaGraph software for the Macintosh.

Fluorescence. Rates of renaturation were determined by the increase in intrinsic tryptophan fluorescence (excitation λ = 300 nm, emission γ = 345 nm). Data were obtained using a SPEX FluoroMax spectrofluorimeter for manual mixing experiments. Alternatively, renaturation rates were monitored with a KinTek Stopped-Flow Model SF2001 (excitation λ = 300 nm, emission 340 nm cutoff filter).

X-ray Crystallography. Large single crystal growth and X-ray diffraction data collection were performed essentially as previously reported (Bryan et al., 1992; Gallagher et al., 1993). The starting model for S22 subtilisin (Table I) was made from the subtilisin BPN′ mutant S12 (Protein Data Bank entry 1SUD).

Data sets with about 20 000 reflections between 8.0- and 1.8-Å resolution were used to refine both models using restrained least-squares techniques (Hendrickson & Konnert, 1980). Initial difference maps for S22 subtilisin, phased by a version of S15 with residues T22 and S87 omitted, showed

[3] The wild-type numbering of amino acids is used for simplicity in defining mutations even when the nine amino acids (75–83) have been deleted.

clear electron density for the disulfide and all omitted atoms. S22 was refined from $R \approx 0.30$ to $R \approx 0.18$ in about 80 cycles, interspersed with calculations of electron density maps and manual adjustments using the graphics modeling program FRODO (Jones, 1978).

RESULTS

Engineering the Disulfide Mutant. The 22–87 disulfide has previously been engineered into subtilisin BPN′ (Pantoliano et al., 1987; Wells et al., 1986). Pantoliano et al reported that the disulfide increased the melting temperature of subtilisin by 3.1 °C relative to that of the wild-type enzyme and 5.8 °C relative to that of the reduced (-SHHS-) form of the mutant.[4] To minimize the effects of the cysteine mutations on the energy of the native state, the sites for insertion of this disulfide cross-link in subtilisin were selected originally in a three-step process (Pantoliano et al., 1987). First, a computer program was used to analyze the 1.3-Å structure of subtilisin (Finzel et al., 1986) for positions where the main-chain atoms of two residues were in the same geometrical relationship as the main-chain atoms in known disulfide linkages taken from the Brookhaven Protein Data Bank. Second, the hypothetical sulfur atoms were inserted into the structure via computer graphics, and those candidates with unfavorable steric interactions were discarded. Third, the amino acid pairs identified were required to be at positions which exhibited some variability in the primary sequence of related subtilisins (Pantoliano et al., 1987). Here this disulfide was introduced into Δ75–83 subtilisin. This allowed us to evaluate the effects of the disulfide on both the unfolding and refolding reactions to determine whether the disulfide cross-link has the anticipated effect on the entropy of the unfolded state. The subtilisins used in this study are defined in Table I. The stabilizing mutations M50F, G169A, Y217K, and N218S were included to partially compensate for the loss of stability due to deletion of site A and make purification of these proteins easier (Bryan et al., 1992; Pantoliano et al., 1989). We have focused our comparisons on C22,C87, Δ75–83 subtilisin S29, with the disulfide in either the reduced or the oxidized state.

X-ray Structure of the Disulfide Cross-Link. The 1.8-Å X-ray structure of S221C subtilisin has been previously reported and was used as the starting model for determining the structure of the T22C–S87C disulfide containing Δ75–83 mutant (Bryan et al., 1992). The structure of C22,C87, Δ75–83 subtilisin is depicted in Figure 1. Analysis of the refined structure reveals that the disulfide bridge is left-handed with $\chi1 = 62°$, $\chi2 = 117°$, $\chi(SS) = -92°$, $\chi2' = 135°$, and $\chi1' = -48°$. The geometry is consistent with that found for another C22,C87 subtilisin variant (Katz & Kossiakoff, 1990). It is interesting to note that without the disulfide bond there are two hydrogen bonds between residues 22 and 87: 22O–87N (2.77 Å) and 2OG1–87OG (2.60 Å). With the disulfide bridge, the 22O–87N (2.93 Å) remains but the second is replaced by the 22SG–87SG covalent bond.

Refolding of Δ75–83 Subtilisin to the Native State. Subtilisin mutants containing the 75–83 deletion can be quantitatively refolded to their native conformations as monitored by several physical criteria:

(1) CD and fluorescence spectra. CD spectra in the far-UV range (Figure 2A), as well as the near-UV (Figure 2B),

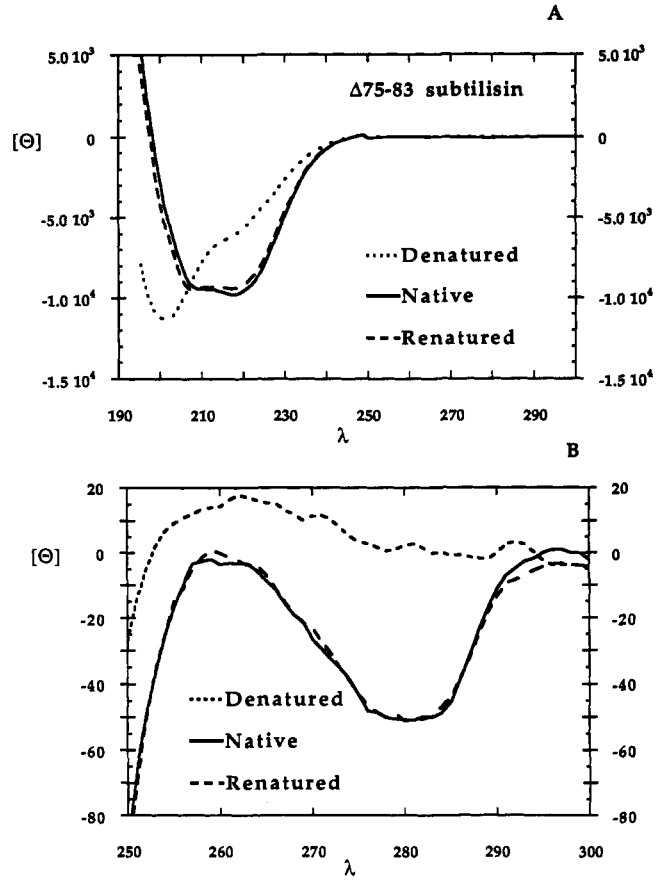

FIGURE 2: CD of native and renatured Δ75–83 subtilisin. (A) Far-UV spectra of native and renatured S15 subtilisin in 0.2 M PO_4, pH 7.2, and denatured S15 subtilisin in 0.1 M PO_4, pH 2.15, are shown. (B) Near-UV spectra of native and renatured S15 subtilisin in 0.2 M PO_4, pH 7.2, and denatured S15 subtilisin in 0.1 M PO_4, pH 2.15, are shown. Mean residue ellipticity is plotted versus wavelength.

and fluorescence emissions spectra of tyrosines and tryptophans are identical in native and renatured subtilisins.

(2) Specific activity. The specific activity of S221C subtilisins against the peptide substrate sAAPFna is ~0.0025 unit/mL (50 000 times less than that of wild-type subtilisin). To demonstrate recovery of peptidase activity in renatured subtilisin, 30 μM Δ75–83 subtilisins were acid-denatured at pH 2.15 and determined to be fully denatured by CD. The samples were then renatured at 0.2 M PO_4, pH 7.2. The refolding reactions were monitored by fluorescence emission at 340 nm and followed to completion. The samples were removed from the fluorescence cell an mixed one-to-one with sAAPFna. The hydrolysis of the substrate was monitored in 0.1 M PO_4, pH 7.2, 0.5 mM sAAPFnA by following the increase in extinction at 410 nm as a function of time. Denatured, uncross-linked Δ75–83 subtilisin recovers ~95% of native specific activity after 30 min of renaturation under these conditions. Denatured Δ75–83 subtilisin S29, which contains the 22–87 cross-link and refolds very rapidly, completely recovers native activity in <1 min of renaturation.

(3) Thermal denaturation. To demonstrate that native and renatured subtilisins are energetically equivalent, thermal denaturation profiles for both were determined by CD. Δ75–83 subtilisins were acid-denatured at pH 2.15 and renatured as described above. The CD spectra of renatured subtilisins were measured and shown to be identical to those of native protein under the same solvent conditions. The native and renatured materials were then melted in the CD and the curves compared. CD melting curves and the derivative curves for

[4] In Pantoliano et al. (1987), DSC of T22C–S87C subtilisin was performed in 50 mM Tris–HCl, pH 8.0, 50 mM KCl, 10 mM EDTA, and 2 mM competitive subtilisin inhibitor Dns–BBA. The triple mutant Y21A, T22C, S87C was reported to be slightly less stable than wild-type subtilisin (Wells & Powers, 1986).

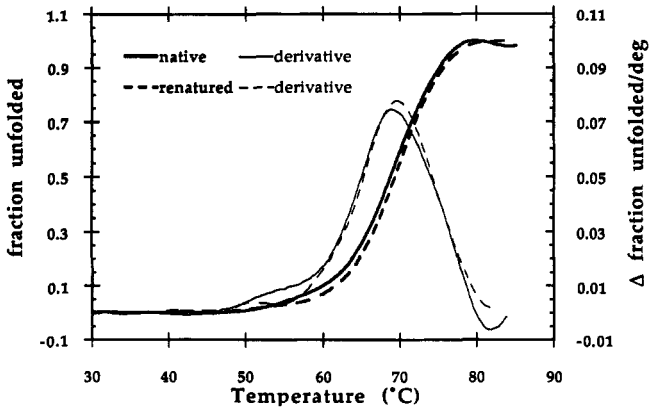

FIGURE 3: CD melting of native and renatured Δ75–83 subtilisin. Subtilisin S15 was renatured as described in the text, and its change in ellipticity at 222 nm was measured as a function of temperature (dashed lines). Melting of native S15 subtilisin is shown for comparison (solid lines). [P] = 1 μM. Cell pathlength was 1 cm. The scan rates were 1 °C/min. The derivative curves (Δfraction unfolded/°C vs temperature) are also shown.

native and renatured Δ75–83 subtilisin are shown in Figure 3. Indistinguishable melting curves for native and renatured subtilisins have been observed for all mutants with the 75–83 deletion.

These results are not consistent with the speculation of Eder et al.(1993) that Δ75–83 subtilisins may not completely refold.

Kinetics of Unfolding. The kinetics of unfolding S29, in the cross-linked and uncross-linked forms, were measured at pH 2.15. CD spectra of Δ75–83 subtilisins taken after 1 min in 0.1 M HPO_4, pH 2.15, indicated that the proteins were unfolded to predominantly random structures. Because the denaturation reaction for Δ75–83 subtilisins is rapid at this pH, the kinetics of unfolding S29 in the cross-linked and uncross-linked forms were measured by stopped-flow mixing methods. Unfolding of S29 subtilisin was monitored by the 15% decrease in fluorescence of its three partially buried tryptophans. S29 in 01. M PO_4, pH 7.0, with and without 0.3 mM reducing agent, DTT, was mixed with two volumes of 0.1 M H_3PO_4. The resulting solution was 0.1 M HPO_4, pH 2.15. The denaturation reactions in both cases can be fit to a single exponential decay with similar rate constants. Denaturation of S29 without DTT is shown in Figure 4A. The residuals after subtraction of the data from the calculated first-order curve are plotted on a 5-times-expanded scale. At 22 °C, k = 14.3 s^{-1} for S29 in 0.1 mM DTT and 10.4 s^{-1} for S29 without DTT.

The temperature dependence of the denaturation rate was also determined over the temperature range of 15–35 °C (Figure 4B). Rates at each temperature were determined by averaging 12–15 experiments. Plots of ln k vs $1/T$ (T = absolute temperature in K) are closely parallel, indicating that the activation energies for unfolding are similar. The absence of obvious curvature in the plots indicates that little change in heat capacity is associated with formation of the transition state for unfolding. ΔC_p for protein unfolding has been shown to be closely correlated with the change in exposure of hydrophobic groups to water (Livingstone et al., 1991; Privalov & Gill, 1988). Since the total heat capacity change for unfolding is 3–4 kcal/deg·mol, the transition state for unfolding at pH 2.15 appears more similar in compactness to that of the native protein than that of the unfolded protein (Chen & Schellman, 1989; Pohl, 1968). The enthalpy of activation of unfolding both cross-linked and uncross-linked S29 at pH 2.15 and 25 °C is ~36 kcal/mol.

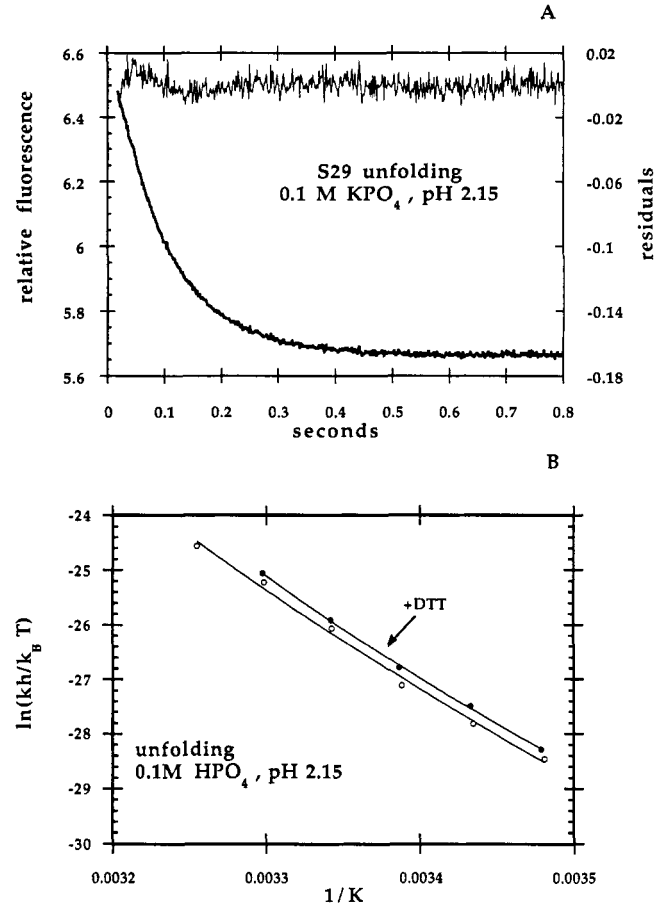

FIGURE 4: Kinetics of unfolding subtilisin S29. (A) Unfolding of S29 in 0.1 M HPO4, pH 2.15 and 22 °C, is followed by the decrease in tryptophan fluorescence. The curve plotted is the average of 12 experiments. The residuals after subtraction of the data from a single exponential fit (k = 10.4 s^{-1}) are plotted on a 5-times-expanded scale. (B) The kinetics of unfolding S29 with and without 1 mM DTT were determined at pH 2.15 over the temperature range of 15–35 °C. The natural log of the apparent equilibrium constant for the transition state ($\ln(kh/k_BT)$) is plotted vs the reciprocal of the absolute temperature.

Kinetics of Folding. Folding rates of the cross-linked and uncross-linked forms of S29 were compared over a range of ionic conditions. At 0.1 M PO_4, both the cross-linked and uncross-linked forms of S29 fold efficiently. Refolding was initiated after a double pH jump. S29 subtilisin (3 μM) was dissolved in 0.05 M PO_4, pH 7.0, either with or without 0.3 mM DTT. Unfolding was induced by the addition of an equal volume of 0.1 M H_3PO_4. The resulting solution had a pH of 2.15. The protein was allowed to denature for 1 s, which was shown above to be sufficient for complete denaturation. After the 1-s delay, the proteins were renatured by the addition of a one-half volume of 0.15 M PO_4, pH 12.0. The resulting solution was 0.1 M PO_4, pH 7.2.

The refolding curves for uncross-linked S29 (in 0.1 mM DTT) at 25 °C are shown in Figure 5. The folding reaction was followed by the 20% increase in tryptophan fluorescence which occurs upon refolding (Figure 5A). Three refolding curves were averaged and fit to a single exponential equation. The calculated first-order rate constant (k_f) equals 0.0027 s^{-1}. The residuals after subtraction of the data from the calculated first-order curve are plotted on a 5-times-expanded scale (Figure 5A). The folding reaction was also monitored by collecting a far-UV CD spectrum (250–200 nm) at 5-min intervals. By 30 min after the second pH jump, the CD spectrum of the renatured S29 was identical to a spectrum of

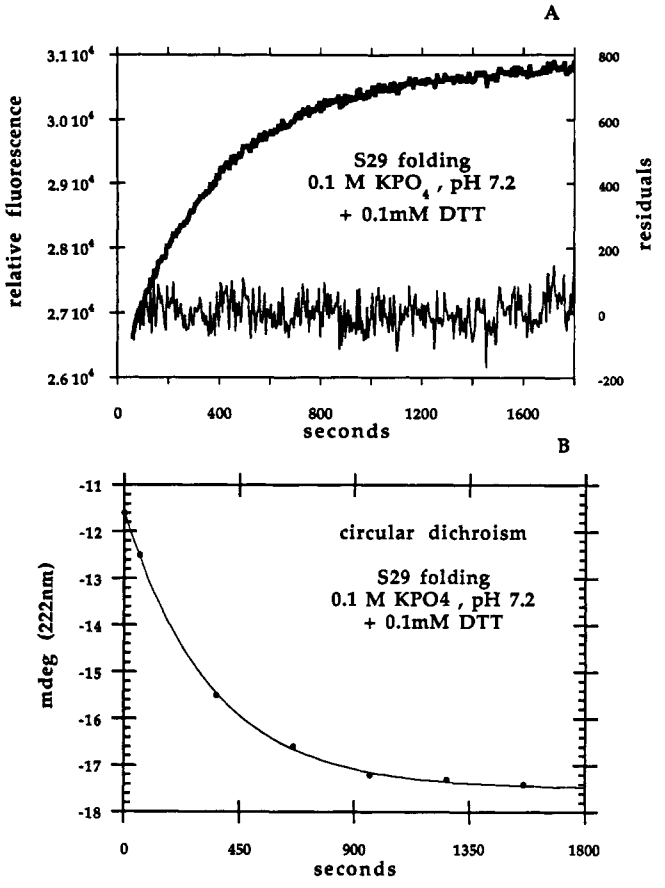

FIGURE 5: Kinetics of refolding uncross-linked S29. (A) Refolding of S29 in 0.1 M KPO_4, pH 7.2, and 0.1 mM DTT at 25 °C, is followed by the increase in tryptophan fluorescence. The curve plotted is the average of three experiments. The residuals after subtraction of the data from a single exponential fit (k = 0.0027 s^{-1}) are plotted on a 5-times-expanded scale. (B) Refolding of S29 in 0.1 M KPO_4, pH 7.2, and 0.1 mM DTT at 25 °C, is followed by CD. Spectra (250–200 nm) were collected at 5-min intervals. The decrease in ellipticity at 222 nm was plotted vs time and fit to a first-order rate equation with k = 0.0027 s^{-1}.

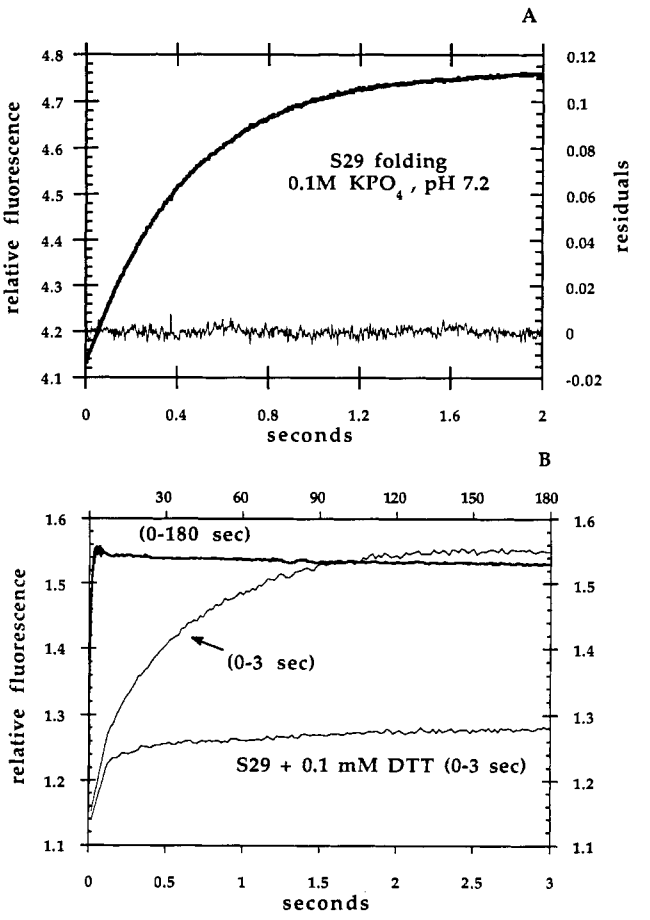

FIGURE 6: Kinetics of refolding S29 in 0.1 M KPO_4, pH 7.2. (A) S29 refolding followed by stopped-flow fluorescence. The curve plotted is the average of 12 experiments. The residuals after subtraction of the data from a single exponential fit (k = 2.3 s^{-1}) are plotted on a 5-times-expanded scale. (B) S29 folding reaction after stopped-flow mixing over two time intervals. 250 data points were collected in the first 3 s, and an additionial 250 data points were collected over the next 180 s, as indicated. For comparison, the folding of uncross-linked S29 was also followed over 3 s after stopped-flow mixing.

native S29 subtilisin. The decrease in ellipticity at 222 nm was plotted vs time and fit to a first-order rate equation with k_f = 0.0027 s^{-1} (Figure 5B).

Measurement of the folding of cross-linked S29 (no DTT) required stopped-flow mixing methods. Refolding was initiated after the same double pH jump described above, but the mixing steps and fluorescence measurements were carried out in a Kintek SF 2001 stopped-flow instrument. The refolding curves for cross-linked S29 at 25 °C are shown in Figure 6A. The folding reaction was followed by a 20% increase in tryptophan fluorescence as above. Twelve refolding curves were averaged and fit to a single exponential equation. The calculated first-order rate constant (k_f) equals 2.3 s^{-1}. The residuals after subtraction of the data from the calculated first-order curve are plotted on a 5-times-expanded scale (Figure 6A). Inspection of residuals indicates that the folding reaction is a single first-order process. The reaction rate for cross-linked S29 under these conditions appeared to be 850 times faster than uncross-linked S29. It was possible, however, that the stopped-flow experiment was measuring a fast folding phase of cross-linked S29, which was then followed by a slower folding phase (Kiefhaber et al., 1992). Manual mixing experiments which measure CD or fluorescence spectra or enzymatic activity indicate that the fully native structure of cross-linked S29 is achieved in <1 min. To span the time interval between 3 s and 1 min, we followed the S29 folding reaction after stopped-flow mixing over two time intervals. In the first 3 s, 250 data points were collected, and an additional 250 data points were collected over the next 180 s (Figure 6B). No slower second phase was detectable by changes in fluorescence. We therefore believe that cross-linked S29 is completely folded at a rate of 2.3 s^{-1}. For comparison, the folding of uncross-linked S29 was also followed over 3 s in the stopped-flow instrument (Figure 6B). A fluorescence change of 2–3% is detectable, with an associated rate of ~20 s^{-1}. The structural interpretation of this small fluorescence change is unclear; however, the result indicates that no major change in the tryptophan environment occurs on a rapid time scale when uncross-linked S29 is returned to native conditions.

The S29 folding reaction was also followed at 0.2 M PO_4, pH 7.2. S29 was dissolved in 0.1 M PO_4, pH 7.0, either with or without 0.3 mM DTT. Refolding was initiated after a double pH jump by the addition of an equal volume of 0.2 M H_3PO_4, followed after 1-s delay by the addition of a one-half volume of 0.3 M PO_4, pH 12.0. The resulting solution is 0.2 M PO_4, pH 7.2. Under both of these conditions, refolding of S29 appears to be a first-order process. Cross-linked S29 folds at a rate of 2.8 s^{-1}. The uncross-linked form folds 700 times slower, at a rate of 0.004 s^{-1} (data not shown).

At low ionic strength, the subtilisin folding reaction is much slower (Bryan et al., 1992). The refolding curves of cross-

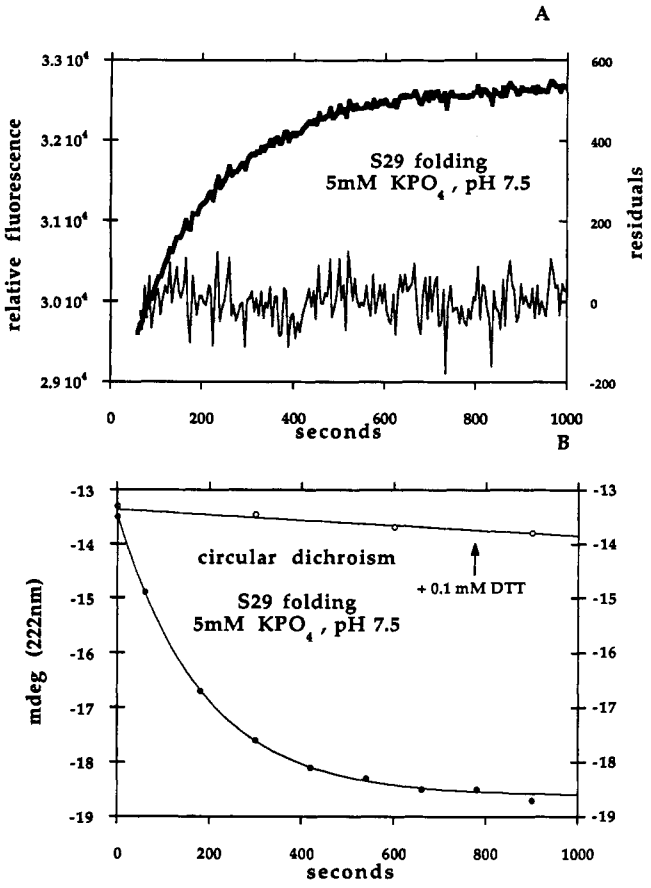

FIGURE 7: Kinetics of refolding S29 at low ionic strength. (A) Refolding of S29 in 30 mM Tris and 5 mM KPO_4, pH 7.5 and 25 °C, is followed by the increase in tryptophan fluorescence. The curve plotted is the average of three experiments. The residuals after subtraction of the data from a single exponential fit ($k = 0.0054\ s^{-1}$) are plotted on a 5-times-expanded scale. (B) Refolding of S29 in 30 mM Tris and 5 mM KPO_4, pH 7.5 and 25 °C, is followed by CD. Spectra (250–200 nm) were collected at 2-min intervals. The increase in ellipticity at 222 nm was plotted vs time and fit to a first-order rate equation with $k = 0.0054\ s^{-1}$.

linked S29, in 30 mM Tris, 5 mM PO_4, pH 7.5, and 25 °C, are shown in Figure 7. S29 was denatured by mixing the protein with HCl in a total volume of 100 μL (pH ≈ 1.8). The final HCl concentration was 0.625 M. All Δ75–83 subtilisin mutants were completely denatured in less than 1 s by these conditions. Acid-denatured S29 was neutralized after ~1 s by diluting 100 μL of denatured protein to 2.5 mL in 30 mM Tris–base and 5 mM PO_4, with rapid stirring (final pH 7.5). The final concentration of subtilisin was 1 μM. The folding reaction was followed by a 20% increase in tryptophan fluorescence (Figure 7A). Three refolding curves were averaged and fit to a single exponential equation. The calculated first-order rate constant (k_f) equals $0.0054\ s^{-1}$. The residuals after subtraction of the data from the calculated first-order curve are plotted on a 5-times-expanded scale (Figure 7A). The folding reaction was also monitored by collecting a far-UV CD spectrum (250–200 nm) at 2-min intervals. By 30 min after the second pH jump, the CD spectrum of the renatured S29 is identical to a spectrum of native S29 subtilisin. The decrease in ellipticity at 222 nm is plotted vs time and fit to a first-order rate equation with $k_f = 0.0054\ s^{-1}$ (Figure 7B).

The folding of S29 in 0.1 mM DTT by CD is shown in Figure 7B. Because of the slow folding of the uncross-linked subtilisin at low ionic strength and the fact that the reaction was only followed for 1 h, only an approximate rate constant was determined. Both fluorescence and CD methods indicate a rate of $< 5 \times 10^{-5}\ s^{-1}$. CD spectra vs time show thatdenatured, uncross-linked subtilisin, when returned to native conditions at low ionic strength, does not rapidly collapse to a molten globule but rather acquires a regular secondary structure at the slow rate of global folding. At 5 mM PO_4, 30 mM Tris–HCl, pH 7.5, and 25 °C, cross-linked S29 folds ≥100 times faster than the uncross-linked form.

DISCUSSION

Decreasing the Entropic Cost of Folding. A disulfide cross-link between residues 22 and 87 was introduced into Δ75–83 subtilisin to determine whether its folding rate could be accelerated by decreasing the entropic cost of ordering the polypeptide chain. If the amino acids 22 and 87 are ordered by the time the transition state is reached in the folding reaction, then the cross-link should accelerate the rate of folding by selectively decreasing the entropy of the unfolded state relative to that of the transition state. For example, chemically cross-linking amino acids 7 and 41 in ribonuclease A has little effect on the kinetics of folding; therefore, this part of the protein was presumed not to be ordered in the transition state (Lin et al., 1985). In contrast, the intrachain disulfide cross-link in the Fc fragment of immunoglobulin light chain significantly accelerates its folding (Goto & Hamaguchi, 1982).

The loss of conformational entropy in a polymer due to a cross-link has been estimated by calculating the probability that the ends of a polymer will simultaneously occur in the same volume element (v_s) according to the equation $\Delta S = -R \ln (3/(2\pi l^2 N)^{3/2}) v_s$ where N is the number of segments and l is the length of a segment (Flory, 1956; Poland & Scheraga, 1965; Schellman, 1955). Good agreement with experimental data for protein cross-linking has been achieved using $l = 3.8$ Å and v_s 58 Å^3, judged to be the closest approach of two –SH groups (Pace et al., 1988). Using these assumptions, the increase in the energy of the unfolded state due to cross-linking 57 amino acids (22 to 87 minus the 9-amino-acid deletion) would be 4.2 kcal/mol at 25 °C. The predicted maximum increase in folding rate at 25 °C would be ~1000-fold. The 22–87 disulfide accelerates folding by 700–850-fold at 25 °C and pH 7.2. Therefore, the acceleration of the folding rate of S29 is qualitatively consistent with a simple statistical mechanical model and suggests that amino acids 22 and 87 are ordered in the transition state for folding.

Nature of the Transition State for Folding. The rates of folding of both the cross-linked and uncross-linked forms of S29 are dependent on ionic conditions. Denatured and uncross-linked Δ75–83 subtilisin, when returned to native conditions at low ionic strength (5 mM PO_4 buffer), remain remarkably devoid of regular secondary structure for hours.

We have suggested previously that the ionic dependence of the folding rate may be related to coalescing the ion-binding site B region of Δ75–83 subtilisin. The region of subtilisin around site B has a high charge density with two Glu, one Asp, one Arg, and one Lys within an 8-Å radius. Particularly striking is the close juxtaposition of E251 and D197. Bringing these charged groups close together in the folding process may be energetically unfavorable. Once these charged residues are arranged in their native conformations with an ion bound, however, they contribute significantly to the stability of the folded state.

Residues 22 and 87 are not in the vicinity of site B (Figure 1), yet both regions of the protein appear to be important in stabilizing the transition state for folding. If protein folding

begins by nucleation of short contiguous regions of polypeptidechain and is propagated by collisions among nucleated regions, then Δ75–83 subtilisin faces two basic problems: (1) many nucleated regions collide with the wrong partners (the entropy problem) and (2) in the case of the ion-binding site B region, the correct partners seldom collide because of unfavorable electrostatics. The first-order kinetics observed for both cross-linked and uncross-linked S29 subtilisin suggest that folding is cooperative. Cooperative folding implies that partially folded intermediate states have low stabilities; thus, multiple, correct collisions of partially folded states must occur almost simultaneously to propagate the folding reaction.

Early organization of the structure around amino acids 22 and 87 due to the cross-link greatly accelerates folding over a range of ionic conditions. We do not know whether the early folding of this region is a highly populated folding pathway in the absence of the cross-link. It is possible that Δ75–83 subtilisin folding could be accelerated by stabilizing a different intermediate structure, which then provides a template to propagate subsequent folding. The slow step in the Δ75–83 subtilisin folding reaction may be forming initial structures capable of propagating folding. Any mutation (or ionic condition) which stabilizes a native-like topology may therefore accelerate the folding rate. Experiments are in progress to test whether cross-links in other regions of subtilisin also result in accelerations of the folding rate.

Stabilization of an early folding nucleus appears to be the mechanism by which the 77-amino-acid subtilisin propeptide catalyzes folding Δ75-83 subtilisin (Strausberg et al., 1993). The rate-limiting step in the reaction of Δ75–83 subtilisin with isolated propeptide appears to be the formation of a productive collision complex between unfolded subtilisin and unfolded propeptide. Following formation of the collision complex, isomerization to the native conformation is rapid.

ACKNOWLEDGMENT

The authors wish to thank Joel Hoskins for synthesizing the oligonucleotides used in site-directed mutagenesis and DNA sequencing; Kathryn Fisher for advice on gene expression and protein production; and Michael Pantoliano, Steven Edwards, John Moult, Matthew Mauro, and Edward Eisenstein for advice and helpful discussion.

REFERENCES

Abrahmsen, L., Tom, J., Burnier, J., Butcher, K. A., Kosiakoff, A., & Wells, J. A. (1991) *Biochemistry 30*, 4151–4159.

Baker, D., Silen, J. L., & Agard, D. A. (1992a) *Proteins: Struct. Funct., Genet. 12*, 339–344.

Baker, D., Sohl, J., & Agard, D. A. (1992b) *Nature 356*, 263–265.

Bryan, P. N. (1992) in *Pharmaceutical Biotechnology* (Ahern, T. J., & Manning, M. C., Eds.) Part B, pp 147–181; Plenum Press, New York.

Bryan, P., Pantoliano, M. W., Quill, S. G., Hsiao, H. Y., & Poulos, T. (1986a) *Proc. Natl. Acad. Sci. U.S.A. 83*, 3743–3745.

Bryan, P., Alexander, P., Strausberg, S., Schwarz, F., Wang, L., Gilliland, G., & Gallagher, D. T. (1992) *Biochemistry 31*, 4937–4945.

Chen, B., & Schellman, J. A. (1989) *Biochemistry 28*, 685–691.

DelMar, E., Largman, C., Brodrick, J., & Geokas, M. (1979) *Anal. Biochem. 99*, 316–320.

Eder, J., Rheinnecker, M., & Fersht, A. R. (1993) *Biochemistry 32*, 18–26.

Finzel, B. C., Howard, A. J., & Pantoliano, M. W. (1986) *J. Cell. Biochem. Suppl. 10A*, 272.

Flory, P. J. (1956) *J. Am. Chem. Soc. 78*, 5222–5235.

Gallagher, T. D., Bryan, P, & Gilliland, G. (1993) *Proteins: Struct. Funct. Genet. 16*, 205–213.

Goto, Y., & Hamaguchi, K. (1982) *J. Mol. Biol.* 891–910.

Hendrickson, W. A., & Konnert, J. H. (1980) in *Computing in Crystallography* (Diamond R., Ranseshan, S., & Venkatesan, K., Eds.), pp 13.01–13.32, Bangalore, Indian Institute of Science.

Ikemura, H., Takagi, H., & Inouye, M. (1987) *J. Biol. Chem. 262*, 7859–7864.

Jones, T. A. (1978) *J. Appl. Crystallogr. 11*, 268–272.

Katz, B., & Kossiakoff, A. A. (1990) *Proteins: Struct. Funct., Genet. 7*, 343–357.

Kiefhaber, T., Schmid, F. Z., Willaert, K., Engleborghs, Y., & Chaffotte, A. (1992) *Protein Sci. 1*, 1162–1172.

Lin, S. H., Konishi, Y., Nall, B., & Scheraga, H. A. (1985) *Biochemistry 24*, 2680–2692.

Livingstone, J. R., Spolar, R. S., & Record, T. M. (1991) *Biochemistry 30*, 4237–4244.

McPhalen, C. A., & James, M. N. G. (1988) *Biochemistry 27*, 6582–6598.

Pace, C. N., Grimsley, G. R., Thomson, J. A., & Barnett, B. J. (1988) *J. Biol. Chem. 264*, 11820–11825.

Pantoliano, M. W., Ladner, R. C., Bryan, P. N., Rollence, M. L., Wood, J. F., & Poulos, T. L. (1987) *Biochemistry 26*, 2077–2082.

Pantoliano, M. W., Whitlow, M., Wood, J. F., Dodd, S. W., Hardman, K. D., Rollence, M. L., & Bryan, P. N. (1989) *Biochemistry 28*, 7205–7213.

Pohl, F. M. (1968) *Eur. J. Biochem. 7*, 146–152.

Poland, D. C., & Scheraga, H. A. (1965) *Biopolymers 3*, 379–399.

Polger, L., & Bender, M. L. (1966) *J. Am. Chem. Soc. 88*, 153–154.

Privalov, P. L., & Gill, S. J. (1988) *Adv. Protein Chem. 39*, 191–234.

Schellman, J. A. (1955) *C. R. Trav. Lab. Carlsberg 29*, 230–259.

Strausberg, S., Alexander, P., Wang, L., Schwarz, F., & Bryan, P. (1993) *Biochemistry 32*, 8112–8119.

Vasantha, N., Thompson, L. D., Rhodes, C., Banner, C., Nagle, J., & Filpula, D. (1984) *J. Bacteriol. 159*, 811–819.

Wells, J. A., & Powers, D. B. (1986) *J. Biol. Chem. 261*, 6564–6570.

Wells, J. A., Ferrari, E., Henner, D. J., Estell, D. A., & Chen, E. Y. (1983) *Nucleic Acids Res. 11*, 7911–7925.

Zhu, X., Ohta, Y., Jordan, F., & Inouye, M. (1989) *Nature 339*, 483–484.